A Magnetic Measurement Plan For The Delta Undulator

Zachary Wolf
SLAC

March 28, 2013

Abstract

This note describes a magnetic measurement plan for the Delta undulator. The note starts by discussing magnetic measurements during assembly of the undulator. The note then discusses measurements of the assembled undulator in detail, including measurments of the field integrals, measurements for calculation of the trajectory, phase, and K value, and undulator fiducialization. Details of the measurements are given so that the note can serve as a reference while the measurements are being made.

1 Introduction[1]

SLAC is building a Delta undulator[2] which will be placed in the LCLS beam line to produce light with variable polarization. A 1 meter prototype is being constructed and a 3.2 meter full length device will be built after the prototype is successfully tested. The period of the undulator is 32 mm.

The ultimate goal of the Delta program at SLAC is to produce an FEL quality undulator. This means that the undulator meets LCLS type tolerances: trajectories are straight at the 2 μm level at 13.5 GeV, first field integrals are below 40 μTm and second integrals are below 50 μTm^2 at all row phases, phase errors are below 10 degrees, K values are known to 10^{-4}, and the undulator is fiducialized with an accuracy of 20 μm. These requirements are summarized in table 1. The measurements to achieve these tolerances are challenging. For LCLS, the undulator had side access allowing the measurement probe position to be controlled by precision granite benches. The Delta has no side access so previous techniques with a granite bench can not be used. The Delta has a 6.6 mm bore through the magnets along its 3.2 m length. All access for the measurements of the assembled undulator must be done in this space. Furthermore, a beam pipe must be in place when the measurements are done due to design constraints. The bore of the beam pipe is 5.0 mm, making the space available smaller. In this note we outline a plan to make the required magnetic measurements in the bore of the undulator. The note discusses the measurements in detail and is intended to be a reference during the measurements. It also suggests areas for future study and development.

2 Basic Assumptions

The techniques outlined in this note for measuring and fiducializing the assembled undulator rely on several basic assumptions. They are given below:

[1] Work supported in part by the DOE Contract DE-AC02-76SF00515. This work was performed in support of the LCLS project at SLAC.

[2] A. Temnykh, Physical Review Special Topics-Accelerators and Beams **11**, 120702 (2008).

Requirement	Value	Units
Trajectory Straightness	< 2	μm
First Field Integrals	< 40	μTm
Second Field Integrals	< 50	μTm^2
Phase Errors	< 10	deg
K Value Accuracy	10^{-4}	
Fiducialization Accuracy	< 20	μm

Table 1: LCLS undulator requirements. These serve as a goal for the Delta program.

1. The magnetic center does not change with the polarization mode of the undulator. In particular, the magnetic center can be found in the linear polarization modes and the center position applies to the circular and elliptical modes.

2. The undulator is well constructed so the magnetic center follows a straight line down the center of the magnet bore at the 100 μm level. Furthermore, the guide tube for the probes and the probe construction keeps the measurement probes near the magnet bore center at the 100 μm level. Combined, the measurement probes stay within about 200 μm of the magnetic center.

3. The harmonic content of the magnetic field within 200 μm of the magnetic center is small. We can use the fundamental term in the field expansion to estimate the field behavior.

These assumptions basically allow us to apply small corrections to the measurements in order to find the fields on the beam axis. The second assumption keeps the level of the corrections at the few parts in 10^4 level. The third assumption implies that if we make a small correction, the error on the correction due to limited knowledge of the fields is second order and can be neglected. For instance, suppose the harmonic terms change the fundamental component of the field by 20%. If we make a correction of 5×10^{-4} based on the fundamental term, the ideal correction is in the range 4×10^{-4} to 6×10^{-4}, so we apply the right correction at the 1×10^{-4} level. These assumptions will play an important role in fiducializing the undulator and determining its K value.

3 Magnetic Measurements Prior To Undulator Assembly

Magnetic measurements must be done at several stages during construction of the undulator. Every magnet block must have its magnetic moment measured in a Helmholtz coil. The blocks are sorted based on the magnetic moment measurements[3]. The purpose of the sorting is to minimize field errors, which will minimize the amount of tuning which must be done on the undulator quadrants. In addition, blocks are chosen and sorted for the undulator ends. These blocks must have modifications done in order to adjust their strength to launch the beam into the undulator center section with no slope and no offset, and similarly to exit with no slope and no offset[4]. The adjusted end blocks are sorted to minimize errors. The sorts produce a list indicating which block goes into each position in the undulator. The blocks are placed into the undulator quadrants following the list.

After the undulator quadrants are assembled, they are measured mechanically to make sure the magnets are placed at the right positions. Based on the mechanical coordinate measuring machine measurements, the blocks are moved closer to the right position. This process is iterated until the block positions are correct to 50 μm.

After the blocks are positioned, magnetic measurements of the quadrants can begin. The quadrants are individually measured both using a Hall probe to measure the magnetic field components,

[3] Z. Wolf, "Delta Undulator Magnet Block Sorting Algorithm", LCLS-TN-13-1, January, 2013.
[4] Z. Wolf, "Delta Undulator End Design", LCLS-TN-13-2, January, 2013.

and also using a moving wire to measure the field integrals. Based on these measurements, individual blocks are moved slightly to change the fields in order to straighten the trajectory, adjust the phase, etc. This process of tuning the quadrants is illustrated in figure 1.

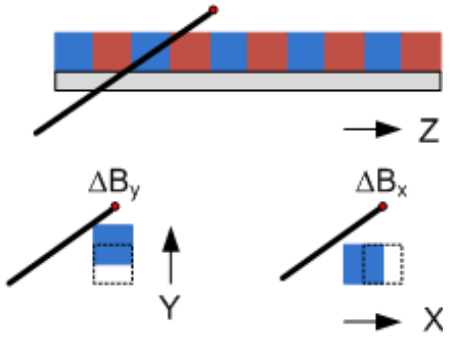

Figure 1: An assembled quadrant is measured by scanning a Hall probe along the quadrant. Vertically magnetized blocks are moved in y to change B_y on axis, and are moved in x to change B_x on axis. Pairs of blocks are moved to make beam offsets and/or adjust phase. Horizontally magnetized blocks are moved to produce phase changes.

If the relative permeability of the blocks was 1, the undulator would be a linear device, and when the four quadrants were assembled to build the undulator, the beam behavior would be the same as the superposition of the behavior from each quadrant. In practice, the relative permeability of the magnet blocks is about 1.05, so the assembled undulator will not be ideal even if each quadrant is tuned to be ideal. The assembled undulator requires further magnetic measurements. This is the subject of the rest of this note. Changes to the assembled undulator are difficult since the quadrants must be disassembled to make an adjustment, and then reassembled and re-measured to check the effect of the adjustment. But it is only after assembly that the magnet block interactions due to permeability effects from neighboring quadrants can be measured.

4 Field Integrals Of The Assembled Undulator

After assembly, the Delta undulator field integrals will be measured with a single stretched wire. A single wire is used to minimize the volume of the field the measurement averages over. Two measurement methods will be used, the moving wire method and the pulsed wire method. One could consider using Hall probes, but they have too much offset drift to give accurate field integrals. They will be used as a consistency check, however.

Both the moving wire and the pulsed wire use the same general setup and the same wire. The wire must be non-magnetic so that there are no forces on it in the magnetic field of the undulator. The wire must also have high tensile strength so that large tension can be applied to minimize sag. The diameter should be small so that the stiffness of the wire does not affect the measurements. On the other hand, the diameter must be large enough so that the wire can be handled. In our experience, 4 mil (100 μm) diameter copper beryllium wire is a good choice. Properties of the wire[5] are listed in table 2.

For the Delta undulator, we assume a typical length of the wire of 5 m. This is a little more than 1.5 times the undulator length, which is required for the pulsed wire measurements so that the reflected wave at the ends does not interfere with the signal. We take the wire tension to be 80% of the 11.4 N maximum tension, or 9.1 N. Given the length of the wire, its electrical resistance will

[5] Little Falls Alloys, Paterson, New Jersey.

Property	Value	Units
Mass density	8.35×10^3	kg/m^3
Resistivity	7.68×10^{-8}	Ωm
Tensile strength	1.4×10^9	N/m^2
Diameter	1.016×10^{-4}	m
Area	8.11×10^{-9}	m^2
Mass per unit length	6.77×10^{-5}	kg/m
Resistance per unit length	9.47	Ω/m
Tension (max)	11.4 [2.57]	N [lbs]

Table 2: Properties of the copper beryllium wire chosen for the measurements.

be 47.4 Ω. If we use a pulser with 487 V amplitude and 50 Ω internal impedance, the current pulse in the wire will have an amplitude of approximately 5.0 A. We summarize these parameters of the measurement system in table 3.

Parameter	Value	Units
Wire length L	5	m
Wire tension T	9	N
Wire mass per unit length m_l	6.77×10^{-5}	kg/m
Gravitational constant g	9.81	m/s^2
Wire current amplitude I_0	5	A

Table 3: Specific parameters of the measurement system.

The fundamental frequency of vibration of the undamped wire is given by

$$f_1 = \frac{1}{2L}\sqrt{\frac{T}{m_l}} \tag{1}$$

Inserting values, we find

$$f_1 = 36.5 \text{ Hz}$$

The wire sag is given by

$$s = \frac{g}{32 f_1^2} \tag{2}$$

Using the value for f_1 and the gravitational constant, we find

$$s = 230 \ \mu\text{m} \tag{3}$$

Note that the wire sag through the undulator is smaller than this value which is over a 5 m length. A sag of 230 μm is not expected to affect the field integrals, however.

4.1 Moving Wire

The moving wire gives both the first and second field integrals. The system is illustrated in figure 2. We now discuss these field integral measurements.

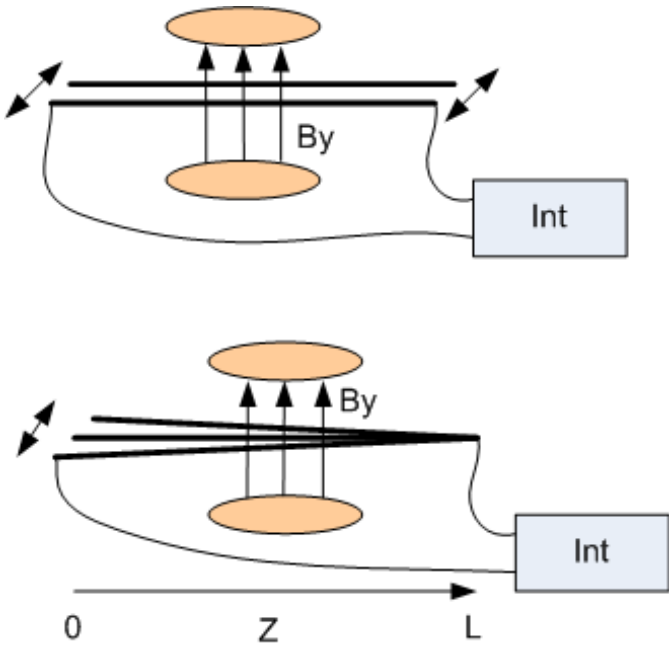

Figure 2: The moving wire technique gives both the first (upper) and second (lower) field integrals.

4.1.1 First Integral

If both ends of the wire are moved horizontally by Δx so that the wire's final position is parallel to its initial position, the flux change in the circuit containing the wire is

$$\Delta\Phi = \Delta \int B_y \, dx \, dz \tag{4}$$

$$= \Delta x \int_0^L B_y \, dz \tag{5}$$

where the integral in z goes over the length of the wire, from the undulator entrance end at $z = 0$ to the exit end at $z = L$. The voltage from the wire is integrated and from Faraday's law, the integral gives the flux change

$$\Delta\Phi = \int V \, dt \tag{6}$$

The limits on the time integral are not specified, but they must extend past the time that the wire is moving. These equations give the field integral in terms of the measured integrated voltage and the measured distance the wire moved.

$$\int_0^L B_y \, dz = \frac{1}{\Delta x} \int V \, dt \tag{7}$$

Similarly, if the wire is moved vertically by Δy and the voltage is integrated, one determines the integral of B_x.

$$\int_0^L B_x \, dz = \frac{1}{\Delta y} \int V \, dt \tag{8}$$

4.1.2 First Integral Signal Estimate

We wish to estimate the signal level for this measurement. Since we want to measure the field uniformity, we must limit the distance we move the wire so that the field structure is not averaged over. Suppose we move the wire 0.5 mm. We wish to measure first field integrals below our tolerance of 40×10^{-6} Tm, so we wish to be able to measure at least 10×10^{-6} Tm. Inserting the distance we move the wire and the minimum field integral we must measure, we find the integrated voltage is

$$\int V\, dt = \Delta x \int_0^L B_y\, dz \tag{9}$$

$$= 5.0 \times 10^{-9} \text{ Vs} \tag{10}$$

The voltage from the wire is sampled and each sample extends over a power line cycle which lasts 0.0167 s. We want at least 10 voltage samples to determine the integrated voltage, so the wire must move at least 0.167 s. The voltage we measure is then the integrated voltage divided by the integration time, which works out to be 30 nV. A very sensitive voltmeter with low offset drift is required. An Agilent 3458 multimeter has 10 nV resolution[6] which is just adequate. The measurements will take place in a laboratory with temperature control to 0.1 °C. If the thermal emf coefficient is 10 μV/°C, thermal voltages will be on the order of 1 μV. This is very large compared to the signal. We will move the wire back and forth, subtract the integrated voltages, and divide by 2 in order to take out the thermal emf. High thermal mass connections that keep the temperature constant over a time period of several seconds must be used so that the thermal emf doesn't change during the two subtracted measurements.

4.1.3 Second Integral

The second integral of B_y if obtained by moving the wire's entrance end at $z = 0$ horizontally by Δx while the exit end at $z = L$ is held stationary. The flux change is given by

$$\Delta\Phi = \int_0^L B_y\, \Delta x \frac{L - z}{L}\, dz \tag{11}$$

$$= \frac{\Delta x}{L} \int_0^L \int_0^z B_y(z')\; dz'\, dz \tag{12}$$

which can be confirmed by integration by parts. The second integral is then given by

$$\int_0^L \int_0^z B_y(z')\; dz'\, dz = \frac{L}{\Delta x} \int V\, dt \tag{13}$$

4.1.4 Second Integral Signal Estimate

The tolerance for the second field integral is 50×10^{-6} Tm^2. We wish to be able to measure better than that, so we take our desired resolution to be 10×10^{-6} Tm^2. The integrated voltage using the 5 m wire with 0.5 mm moves at the entrance end is then

$$\int V\, dt = \frac{\Delta x}{L} \int_0^L \int_0^z B_y(z')\; dz'\, dz \tag{14}$$

$$= 1.0 \times 10^{-9} \text{ Vs} \tag{15}$$

The measurement is more difficult than the measurement of the first integral. The integrated voltage is 1/5 as large, so the voltage is 6 nV instead of 30 nV. At least 1 mm wire motion at the entrance end will be required.

[6] "Agilent 3458A Multimeter Data Sheet", Agilent Corp., www.agilent.com.

4.2 Pulsed Wire

The pulsed wire[7] is used to confirm the moving wire measurements. Typically, the pulsed wire measurement is noisier than the moving wire measurement, but it provides a valuable independent check. The pulsed wire system is illustrated in figure 3. A current pulse is applied to the wire. The magnetic field along the wire interacts with the current pulse to give the wire an initial velocity. The transverse wire motion moves as a wave longitudinally along the wire and is detected by a sensitive detector. A calibration magnet is used to put a known field integral into the measured signal. The details of how this works are described below.

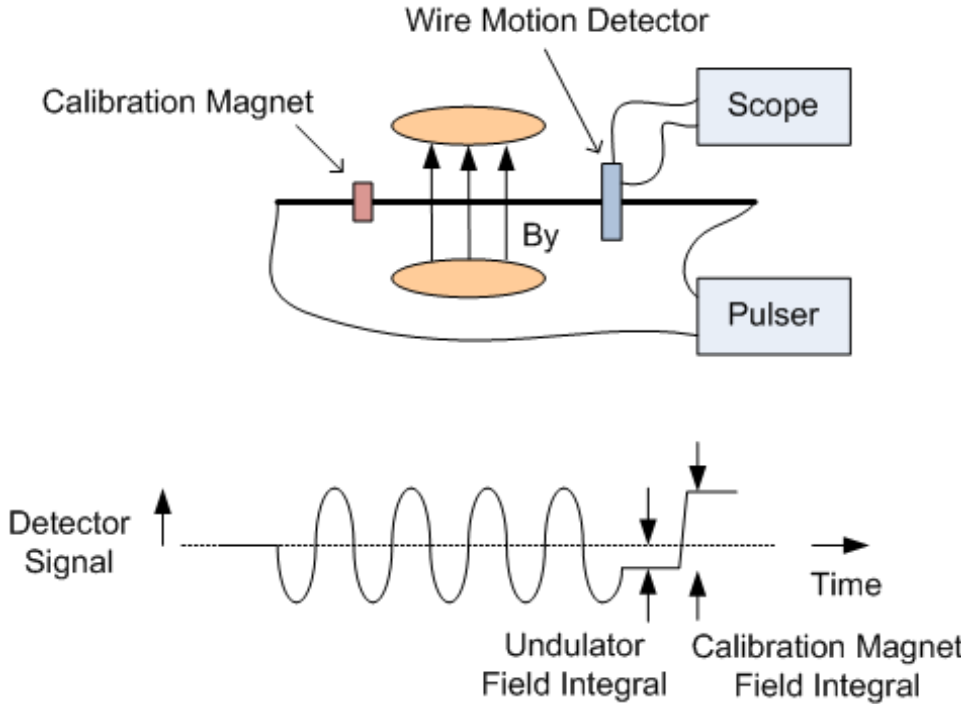

Figure 3: Illustration of the pulsed wire setup and the signal on the wire motion detector.

4.2.1 First Integral

To measure the first field integral, a current pulse of amplitude I_0 and of duration Δt is applied to the wire. We make the pulse duration Δt short so that the wire does not move significantly during the pulse The wire is assumed to be stationary before the pulse and at location $x = 0$ and $y = 0$. The current pulse then gives the wire an impulse per unit length given by

$$p_l(z) = \int f_l(z,t)\, dt \tag{16}$$

where f_l is the force per unit length and p_l is the momentum per unit length in the direction of the force. The force per unit length in the x direction from a vertical field B_y and current I in the $-z$ direction is given by

$$f_l(z,t) = I(t)\, B_y(z) \tag{17}$$

[7] R. Warren, "Limitations on the Use of the Pulsed-Wire Field Measuring Technique", NIM A272 (1988) 257.

and the integral of the force is given by

$$\int f_l(z,t)\,dt = \int I(t)\,B_y(z)\,dt \tag{18}$$

$$= I_0 \Delta t B_y(z) \tag{19}$$

The momentum per unit length p_{lx} in the x direction is given by

$$p_{lx}(z) = m_l v_x(z) \tag{20}$$

where m_l is the mass per unit length of the wire and v_x is the velocity of the wire in the x direction after the current pulse. Equating the momentum change to the impulse, we find

$$m_l v_x(z) = I_0 \Delta t B_y(z) \tag{21}$$

or

$$v_x(z) = \frac{1}{m_l} I_0 \Delta t B_y(z) \tag{22}$$

This initial velocity causes a wave to propagate in both the $+z$ and $-z$ directions down the wire with velocity c, where

$$c = \sqrt{\frac{T}{m_l}} \tag{23}$$

where T is the wire tension. The displacement of the wire is the sum of the displacements from the wave travelling toward $+z$ and the wave travelling toward $-z$.

$$x_{tot}(z,t) = x_-(z+ct) + x_+(z-ct) \tag{24}$$

The velocity of the wire is given by

$$v_{xtot}(z,t) = v_{x-}(z+ct) + v_{x+}(z-ct) \tag{25}$$

By symmetry, half the initial transverse wire velocity goes into the wave moving toward $+z$, and half into the wave moving toward $-z$.

Consider only the wave propagating in the negative z direction toward the detector at $z = 0$. It's amplitude is given by

$$x(z,t) = x(z+ct) \tag{26}$$

The velocity of the wave is

$$v_x(z,t) = x'(z+ct)\,c \tag{27}$$

where the prime indicates a derivative with respect to the function's argument. The wire velocity at $t = 0^+$ after the impulse has been calculated in equation 22. Including a factor of $1/2$ to account for half the initial wire motion going into the backward wave, we find

$$v_x(z,0) = x'(z)\,c = \frac{1}{2m_l} I_0 \Delta t B_y(z) \tag{28}$$

So

$$x'(z) = \frac{1}{2cm_l} I_0 \Delta t B_y(z) \tag{29}$$

Integrating, we find

$$x(\zeta) = \frac{1}{2cm_l} I_0 \Delta t \int_0^{\zeta} B_y(z')\,dz' \tag{30}$$

or

$$x\left(z,t\right)=\frac{1}{2cm_l}I_0\Delta t\int_0^{z+ct}B_y\left(z'\right)dz' \tag{31}$$

The wire displacement at the detector at $z=0$ is given by

$$x\left(0,t\right)=\frac{1}{2cm_l}I_0\Delta t\int_0^{ct}B_y\left(z'\right)dz' \tag{32}$$

By measuring the wire displacement as a function of time, we determine the field integral

$$\int_0^z B_y\left(z'\right)dz'=\frac{2cm_l}{I_0\Delta t}\,x\left(0,t=\frac{z}{c}\right) \tag{33}$$

4.2.2 First Integral Signal Estimate

We can estimate the amplitude of the wire motion using the parameters of the wire and the tolerance on the undulator field integral. We use the full tolerance value for the field integral since we are only using the pulsed wire to check the moving wire measurements. The speed of a wave on the wire is given by

$$c=\sqrt{\frac{T}{m_l}} \tag{34}$$

Using $T=9$ N and $m_l=6.77\times10^{-5}$ kg/m, we find

$$c=365\text{ m/s} \tag{35}$$

We must choose the current pulse width so that the signal is measurable, but also so that the response wave propagates only a small distance compared to the undulator period during the pulse. We take $\Delta t=20\times10^{-6}$ s. Then $c\Delta t=7.3\times10^{-3}$ m, which is smaller than the 32×10^{-3} m undulator period, but not significantly smaller. Using $I_0=5$ A, and $\int_0^L B_y\left(z'\right)dz'=40\times10^{-6}$ Tm, we find

$$\begin{aligned} x\left(0,t=\frac{L}{c}\right) &= \frac{I_0\Delta t}{2cm_l}\int_0^{ct}B_y\left(z'\right)dz' && (36)\\ &= 0.08\ \mu\text{m} && (37)\end{aligned}$$

This is a very small wire motion, so a sensitive detector must be used. A suitable detector was developed and successfully used for the LCLS quadrupole fiducialization[8]. Because the wire motion is small, unwanted vibrations of the wire must be kept to a minimum.

A calibration magnet is included in the data set giving the wire displacement for a known field integral. This allows the undulator field integral to be determined easily without having to accurately know the wire parameters and wire motion detector sensitivity.

4.2.3 Second Integral

The second integral of the field is obtained by applying a current step function to the wire instead of the short pulse used for the first integral. The step function can be thought of as a series of pulses. Let $P(t)$ be a pulse of amplitude 1 at time t of duration Δt. Then

$$\begin{aligned} I(t) &= I_0P(0)+I_0P(\Delta t)+I_0P(2\Delta t)+I_0P(3\Delta t)+... && (38)\\ &= \sum_{n=0}^{\infty}I_0P(n\Delta t) && (39)\end{aligned}$$

[8] Z. Wolf, "A Vibrating Wire System For Quadrupole Fiducialization", LCLS-TN-05-11, May, 2005.

By superposition, the wire displacement at the detector is given by

$$\chi(0,t) = \sum_{n=0}^{t/\Delta t} x(0, t - n\Delta t) \tag{40}$$

Let $\tau = n\Delta t$. Then

$$\chi(0,t) \simeq \int_0^t \frac{d\tau}{\Delta t} x(0, t-\tau) \tag{41}$$

Substituting the pulse response and taking the limit of Δt small, we get

$$\chi(0,t) = \int_0^t \frac{d\tau}{\Delta t} \frac{1}{2cm_l} I_0 \Delta t \int_0^{c(t-\tau)} B_y(z')\, dz' \tag{42}$$

Let $z = ct$, and $\zeta = c\tau$. Then

$$\chi\left(0, t = \frac{z}{c}\right) = \int_0^z \frac{d\zeta}{c} \frac{1}{2cm_l} I_0 \int_0^{z-\zeta} B_y(z')\, dz' \tag{43}$$

Let $z'' = z - \zeta$. Then

$$\chi\left(0, t = \frac{z}{c}\right) = \int_z^0 \frac{-dz''}{c} \frac{1}{2cm_l} I_0 \int_0^{z''} B_y(z')\, dz' \tag{44}$$

or

$$\chi\left(0, t = \frac{z}{c}\right) = \frac{I_0}{2c^2 m_l} \int_0^z \int_0^{z''} B_y(z')\, dz' dz'' \tag{45}$$

This expression lets us determine the second integral of the field by looking at the wire displacement when a current step function is applied to the wire.

$$\int_0^z \int_0^{z''} B_y(z')\, dz' dz'' = \frac{2c^2 m_l}{I_0} \chi\left(0, t = \frac{z}{c}\right) \tag{46}$$

4.2.4 Second Integral Signal Estimate

We can estimate the amplitude of the wire motion using the parameters given above when considering the first integral. For a second integral equal to the tolerance limit of 50×10^{-6} Tm^2, we find

$$\begin{aligned} \chi\left(0, t = \frac{L}{c}\right) &= \frac{I_0}{2c^2 m_l} \int_0^L \int_0^{z''} B_y(z')\, dz' dz'' \\ &= 13.9\ \mu\text{m} \end{aligned} \tag{47}$$

This is a large signal, and in fact the current would have to be reduced with the present wire motion detector in order to make this measurement.

5 Calculation Of Fields In The Undulator

For the remaining measurements of this note, we need to know the behavior of the fields in the undulator. In this section, we first find an analytic expression for the scalar potential of the fields. We then simplify the general expression by using only the dominant fundamental term in the expansion. The dominant term is used to explicitly calculate the fields in the linear and circular polarization modes. Finally, a simulation of the undulator is used to estimate values for the free parameters.

5.1 Analytic Expression

For this calculation, we assume the origin of the coordinate system in x and y is at the magnetic center of the fields. The magnetic field in the bore of the undulator obeys the following equations.

$$\nabla \times B = 0 \tag{48}$$
$$\nabla \cdot B = 0 \tag{49}$$

Since the curl of B is zero, B can be expressed in terms of a scalar potential, $B = \nabla\phi$. The scalar potential obeys Laplace's equation.

$$\nabla^2\phi = 0 \tag{50}$$

To solve this equation, we use separation of variables.

$$\phi = X(x)Y(y)Z(z) \tag{51}$$

Laplace's equation becomes

$$\frac{X''}{X} + \frac{Y''}{Y} + \frac{Z''}{Z} = 0 \tag{52}$$

Since the sum of terms each containing a different independent variable is zero, each term must be a constant, and the sum of the constants must be zero.

$$\frac{X''}{X} = k_x^2 \tag{53}$$
$$\frac{Y''}{Y} = k_y^2 \tag{54}$$
$$\frac{Z''}{Z} = k_z^2 \tag{55}$$
$$k_x^2 + k_y^2 + k_z^2 = 0 \tag{56}$$

We only consider solutions periodic in z with multiples of the undulator period in the body of the undulator. k_z is imaginary.

$$Z_n(z) = c_5(n)\cos(nk_u z) + c_6(n)\sin(nk_u z) \tag{57}$$

where n in an integer, $c_5(n)$ and $c_6(n)$ are constants that depend on the row phase of the undulator, and $k_u = 2\pi/\lambda_u$ where λ_u is the undulator period. The X and Y terms have no periodicity requirements.

$$X_{k_x}(x) = c_1(k_x)\cosh(k_x x) + c_2(k_x)\sinh(k_x x) \tag{58}$$
$$Y_{k_y}(y) = c_3(k_y)\cosh(k_y y) + c_4(k_y)\sinh(k_y y) \tag{59}$$

The general form of the potential is

$$\begin{aligned}\phi = \sum_{n=0}^{\infty} \iint_{\Omega} dk_x dk_y \{&[c_1(k_x)\cosh(k_x x) + c_2(k_x)\sinh(k_x x)] \\ &\times [c_3(k_y)\cosh(k_y y) + c_4(k_y)\sinh(k_y y)]\,[c_5(n)\cos(nk_u z) + c_6(n)\sin(nk_u z)]\}\end{aligned} \tag{60}$$

where the region of integration Ω is over all values of k_x and k_y, real and complex, that satisfy

$$k_x^2 + k_y^2 - n^2 k_u^2 = 0 \tag{61}$$

We will only consider this solution near $x = 0$ and $y = 0$. We approximate the field by using only the dominant term in this region. It will contain the first harmonic with $n = 1$. So

$$Z(z) = c_5\cos(k_u z) + c_6\sin(k_u z) \tag{62}$$

The values of k_x and k_y are still free within the constraint. We leave k_x and k_y as parameters in the expression for the potential. With these considerations, the scalar potential has the form

$$\begin{aligned}\phi &= [c_1 \cosh(k_x x) + c_2 \sinh(k_x x)] \\ &\quad \times [c_3 \cosh(k_y y) + c_4 \sinh(k_y y)] \\ &\quad \times [c_5 \cos(k_u z) + c_6 \sin(k_u z)] \end{aligned} \tag{63}$$

where the c_i are constants. The parameters k_x, k_y, and k_u have the constraint

$$k_x^2 + k_y^2 = k_u^2 \tag{64}$$

We use this form of the potential to calculate the fields. We do this explicitly for the two linear and two circular polarization modes. For ease of notation, some of the same symbols are used when analyzing each mode, but they take on different values for the different modes.

5.1.1 Linear Polarization Vertical Field

Consider the linear polarization vertical field mode. The magnet arrays are illustrated in the upper part of figure 4. At $z = 0$ the field is toward $+y$. There is forward-backward symmetry of the potential in z. There is left-right symmetry in x. The scalar potential increases monotonically as one moves up in y. The potential that satisfies these boundary conditions is

$$\phi = c_1 \cosh(k_x x) \times c_4 \sinh(k_y y) \times c_5 \cos(k_u z) \tag{65}$$

Letting $\phi_0 = c_1 c_4 c_5$, the fields are

$$B_x = \phi_0 k_x \sinh(k_x x) \sinh(k_y y) \cos(k_u z) \tag{66}$$

$$B_y = \phi_0 k_y \cosh(k_x x) \cosh(k_y y) \cos(k_u z) \tag{67}$$

$$B_z = -\phi_0 k_u \cosh(k_x x) \sinh(k_y y) \sin(k_u z) \tag{68}$$

Note that in a planar undulator with wide poles, $k_x = 0$ and $k_y = k_u$. We recover the conventional form of the fields.

5.1.2 Linear Polarization Horizontal Field

Now consider the linear polarization horizontal field mode of the undulator. This is shown in the lower part of figure 4. At $z = 0$ the field is toward $+x$. There is forward-backward symmetry of the potential in z. There is top-bottom symmetry in y. The scalar potential increases monotonically as one moves toward $+x$. The potential that satisfies these boundary conditions is

$$\phi = c_2 \sinh(k_x x) \times c_3 \cosh(k_y y) \times c_5 \cos(k_u z) \tag{69}$$

Letting $\phi_0 = c_2 c_3 c_5$, the fields are

$$B_x = \phi_0 k_x \cosh(k_x x) \cosh(k_y y) \cos(k_u z) \tag{70}$$

$$B_y = \phi_0 k_y \sinh(k_x x) \sinh(k_y y) \cos(k_u z) \tag{71}$$

$$B_z = -\phi_0 k_u \sinh(k_x x) \cosh(k_y y) \sin(k_u z) \tag{72}$$

In a planar undulator with wide poles, $k_y = 0$, $k_x = k_u$, and we recover the conventional form of the fields.

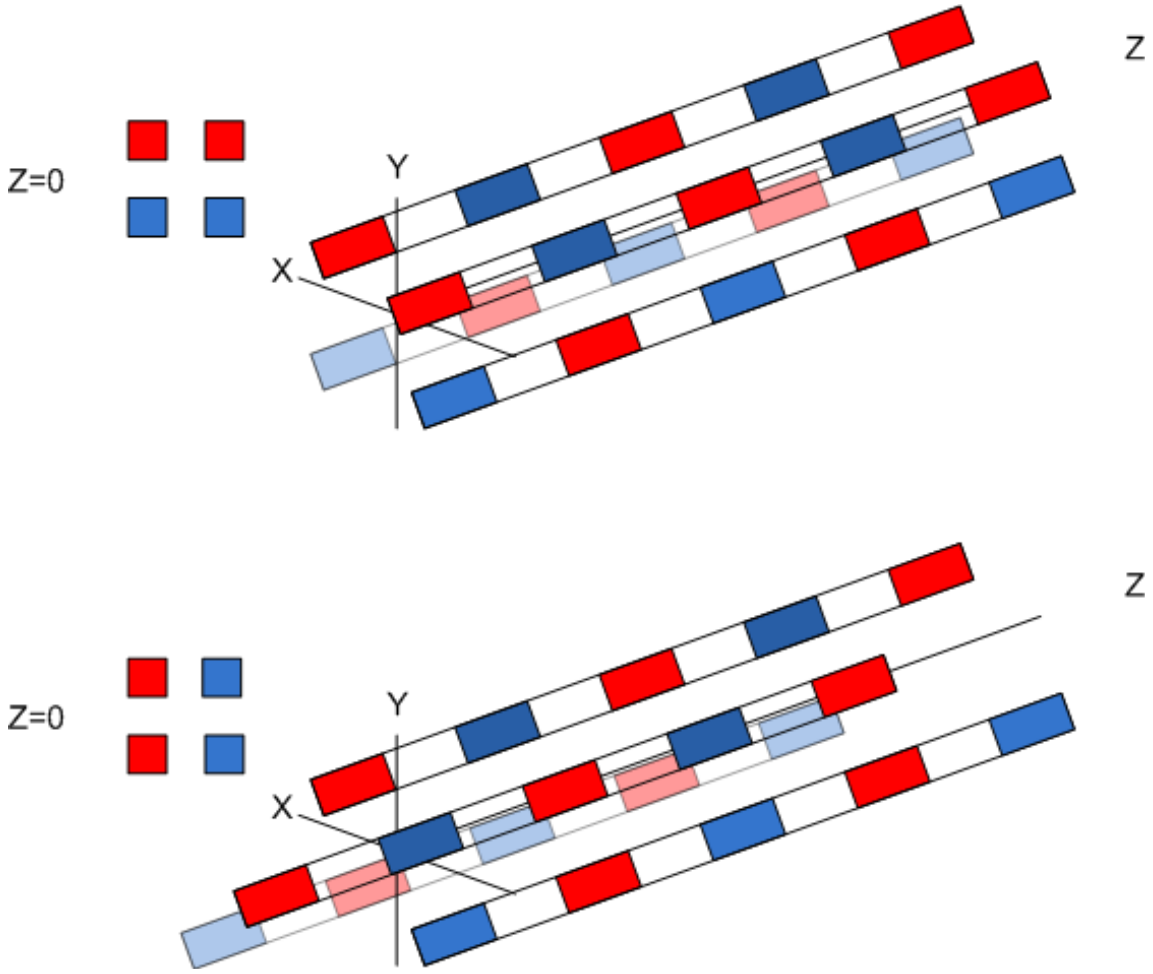

Figure 4: Linear polarization vertical field mode (upper) and horizontal field mode (lower).

5.1.3 Circular Right Handed Polarization[9]

Consider the undulator in right handed circular polarization mode. The arrays are arranged as shown in figure 5. In order to calculate the fields, we use superposition and divide the undulator into a periodic part that starts at $z = 0$, and a periodic part that starts at $z = \lambda_u/4$. We further use superposition to express the potential at $z = 0$ and at $z = \lambda_u/4$ as the sum of the potentials from two equal strength planar undulators. This is illustrated in the lower part of figure 5. At $z = 0$, the planar undulators have fields in the $+y$ and $+x$ directions, both of which we have already seen. At $z = \lambda_u/4$, the planar undulators have fields in the $+y$ and $-x$ directions. The scalar

[9] The techniques in this section were motivated by R. Schlueter and S. Prestemon, "Magnetic Systems: Insertion Device Design", USPAS, Winter 2008.

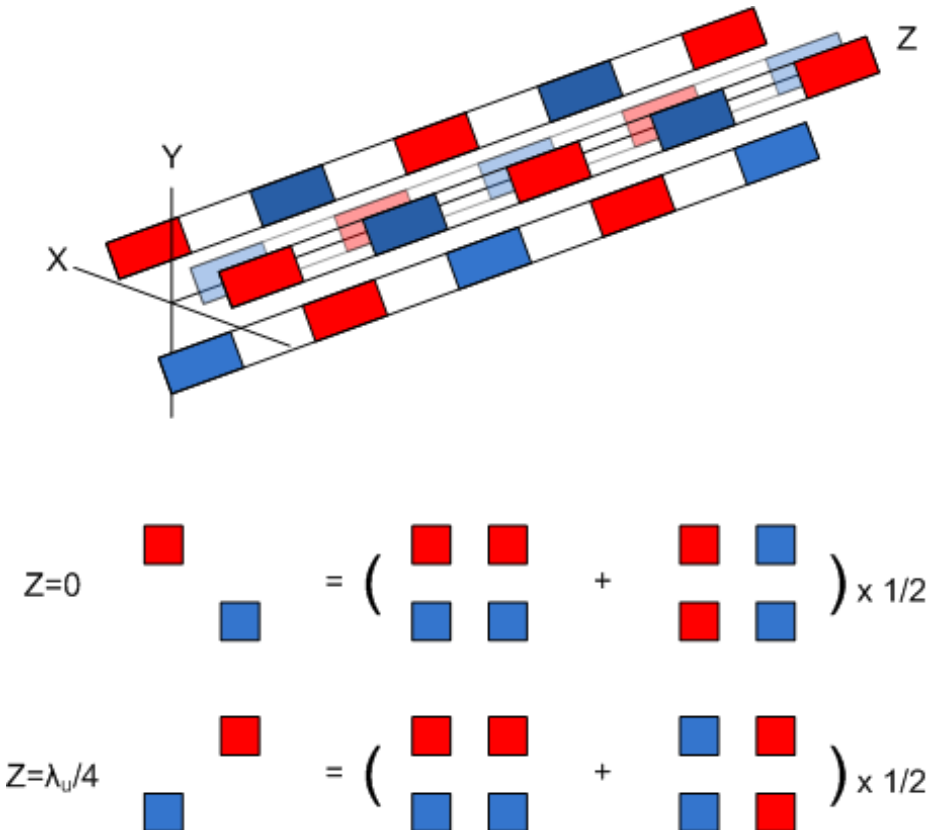

Figure 5: Configuration of the undulator in right handed circular polarization mode.

potential, using the previous results, is then

$$\begin{aligned}\phi &= \frac{1}{2}\phi_0\left[\cosh\left(k_x x\right)\sinh\left(k_y y\right)\cos\left(k_u z\right)+\sinh\left(k_x x\right)\cosh\left(k_y y\right)\cos\left(k_u z\right)\right]\\ &+\frac{1}{2}\overline{\phi_0}[\cosh\left(k_x x\right)\sinh\left(k_y y\right)\cos\left(k_u\left(z-\lambda_u/4\right)\right)\\ &-\sinh\left(k_x x\right)\cosh\left(k_y y\right)\cos k_u\left(z-\lambda_u/4\right)]\end{aligned} \tag{73}$$

For circular polarization, we have $\phi_0 = \overline{\phi_0}$. Since $k_u\lambda_u/4 = \pi/2$, and $\cos(k_u z - \pi/2) = \sin(k_u z)$, we have

$$\begin{aligned}\phi &= \frac{1}{2}\phi_0\left[\cosh\left(k_x x\right)\sinh\left(k_y y\right)+\sinh\left(k_x x\right)\cosh\left(k_y y\right)\right]\cos\left(k_u z\right)\\ &+\frac{1}{2}\phi_0\left[\cosh\left(k_x x\right)\sinh\left(k_y y\right)-\sinh\left(k_x x\right)\cosh\left(k_y y\right)\right]\sin\left(k_u z\right)\end{aligned} \tag{74}$$

Using trigonometric identities, we have

$$\phi = \frac{1}{2}\phi_0\sinh\left(k_x x+k_y y\right)\cos\left(k_u z\right)-\frac{1}{2}\phi_0\sinh\left(k_x x-k_y y\right)\sin\left(k_u z\right) \tag{75}$$

By symmetry, $k_x = k_y$. Since $k_x^2 + k_y^2 = k_u^2$, $k_x = k_y = \frac{1}{\sqrt{2}}k_u$.

$$\phi = \frac{1}{2}\phi_0\sinh\left(\frac{1}{\sqrt{2}}k_u(x+y)\right)\cos\left(k_u z\right)-\frac{1}{2}\phi_0\sinh\left(\frac{1}{\sqrt{2}}k_u(x-y)\right)\sin\left(k_u z\right) \tag{76}$$

The fields are

$$\begin{aligned} B_x &= \frac{1}{2\sqrt{2}}\phi_0 k_u \cosh\left(\frac{1}{\sqrt{2}}k_u(x+y)\right)\cos\left(k_u z\right) \\ &\quad -\frac{1}{2\sqrt{2}}\phi_0 k_u \cosh\left(\frac{1}{\sqrt{2}}k_u(x-y)\right)\sin\left(k_u z\right) \qquad (77) \\ B_y &= \frac{1}{2\sqrt{2}}\phi_0 k_u \cosh\left(\frac{1}{\sqrt{2}}k_u(x+y)\right)\cos\left(k_u z\right) \\ &\quad +\frac{1}{2\sqrt{2}}\phi_0 k_u \cosh\left(\frac{1}{\sqrt{2}}k_u(x-y)\right)\sin\left(k_u z\right) \qquad (78) \\ B_z &= -\frac{1}{2}\phi_0 k_u \sinh\left(\frac{1}{\sqrt{2}}k_u(x+y)\right)\sin\left(k_u z\right) \\ &\quad -\frac{1}{2}\phi_0 k_u \sinh\left(\frac{1}{\sqrt{2}}k_u(x-y)\right)\cos\left(k_u z\right) \qquad (79) \end{aligned}$$

5.1.4 Circular Left Handed Polarization

For circular left handed polarization, the fields at $z = \lambda_u/4$ are reversed compared to the case of circular right handed polarization. The scalar potential is then

$$\phi = \frac{1}{2}\phi_0 \sinh\left(\frac{1}{\sqrt{2}}k_u(x+y)\right)\cos\left(k_u z\right) + \frac{1}{2}\phi_0 \sinh\left(\frac{1}{\sqrt{2}}k_u(x-y)\right)\sin\left(k_u z\right) \qquad (80)$$

The fields are

$$\begin{aligned} B_x &= \frac{1}{2\sqrt{2}}\phi_0 k_u \cosh\left(\frac{1}{\sqrt{2}}k_u(x+y)\right)\cos\left(k_u z\right) \\ &\quad +\frac{1}{2\sqrt{2}}\phi_0 k_u \cosh\left(\frac{1}{\sqrt{2}}k_u(x-y)\right)\sin\left(k_u z\right) \qquad (81) \\ B_y &= \frac{1}{2\sqrt{2}}\phi_0 k_u \cosh\left(\frac{1}{\sqrt{2}}k_u(x+y)\right)\cos\left(k_u z\right) \\ &\quad -\frac{1}{2\sqrt{2}}\phi_0 k_u \cosh\left(\frac{1}{\sqrt{2}}k_u(x-y)\right)\sin\left(k_u z\right) \qquad (82) \\ B_z &= -\frac{1}{2}\phi_0 k_u \sinh\left(\frac{1}{\sqrt{2}}k_u(x+y)\right)\sin\left(k_u z\right) \\ &\quad +\frac{1}{2}\phi_0 k_u \sinh\left(\frac{1}{\sqrt{2}}k_u(x-y)\right)\cos\left(k_u z\right) \qquad (83) \end{aligned}$$

5.2 Modeled Fields

In the planar polarization modes, the expressions for the fields have free parameters k_x and k_y. The fields in the undulator were modeled[10]. We use results from modeling the undulator to estimate the values for these parameters.

The field variation in the x-direction when the undulator was in the vertical field mode is shown in figure 6, and the field variation in the y-direction is shown in figure 7. The form of the B_y field is

$$B_y = \phi_0 k_y \cosh\left(k_x x\right)\cosh\left(k_y y\right)\cos\left(k_u z\right)$$

The x-variation of the modeled field was fit with a hyperbolic cosine giving $k_x = 0.222$ 1/mm. The

[10] This work was done by Alexander Temnykh of Cornell.

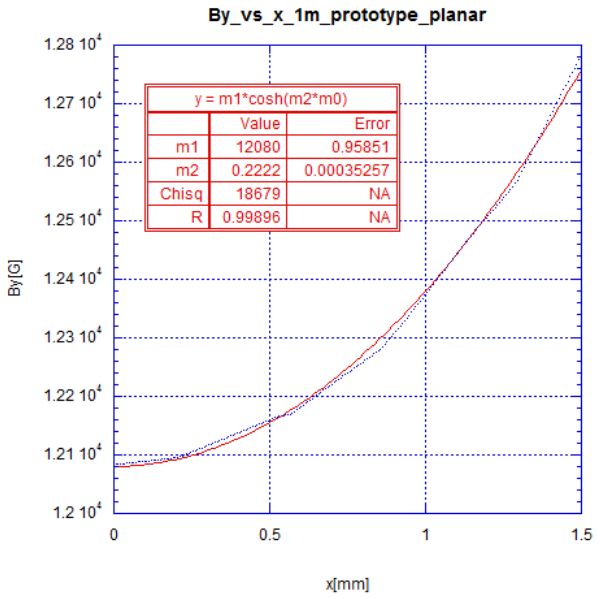

Figure 6: Simulation of the Delta undulator in the vertical field mode showing how the field B_y varies with x.

y-variation of the field was fit with a cosine function giving $k_y = i0.129$ 1/mm Note that k_y is imaginary and the field variation is locally concave down.

Since $k_u = 2\pi/\lambda_u$, and the undulator period is $\lambda_u = 32$ mm, $k_u = 0.196$ 1/mm. We check the constraint by comparing $k_x^2 + k_y^2$ to k_u^2.

$$k_x^2 + k_y^2 = 0.0326 \text{ 1/mm}^2 \quad (84)$$

$$k_u^2 = 0.0384 \text{ 1/mm}^2 \quad (85)$$

The constraint is roughly satisfied. The discrepancy may be due to the fact that the fundamental term in the expansion may not sufficiently describe the field over the large range of the fits. We will determine k_x and k_y from the measurements, but the model gives a good idea of what to expect.

When the undulator is in planar horizontal field mode, we found that the form of the B_x field is

$$B_x = \phi_0 k_x \cosh(k_x x) \cosh(k_y y) \cos(k_u z)$$

By symmetry, in this mode the modeled parameters are $k_x = i0.129$ 1/mm and $k_y = 0.222$ 1/mm.

6 Measurement Of The Fields In The Undulator

The undulator characteristics such as trajectories, phase, and K value will be calculated from Hall probe measurements of the magnetic field. Since the fields vary with position, the measurement depends on where the probe is and also on where the unknown magnetic center is. There is no way to position the probe so the measurements take place at a magnetic center or at a beam axis location. The probe position must be determined both transversely and longitudinally in the undulator bore. The position of the magnetic center relative to the probes must be combined with the probe position in order to give the magnetic center position. To fully characterize the fields, we must also measure k_x, k_y, and the field amplitude at the magnetic center. In this section we discuss how we plan to

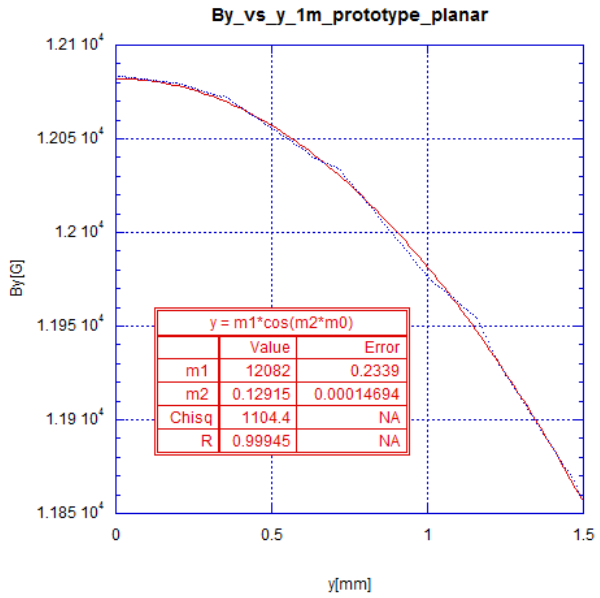

Figure 7: Simulation of the Delta undulator in the vertical field mode showing how the field B_y varies with y.

measure the magnetic field, determine the field parameters from the measurements, determine the beam axis from the measurements, relate the beam axis to fiducials on the undulator, and determine the undulator parameters such as trajectories and phase on the beam axis.

It turns out that we only have room in the undulator bore for two Hall probes. We offset the probes in one direction, thus we sample the field at two points in the offset direction[11]. The probe can be rotated, however, to rotate the offset direction. We must use this limited set of measurements to determine the undulator parameters.

6.1 Hall Probes

Both B_x and B_y must be determined in the presence of all three field components. Hall probes typically have crosstalk between the components. To minimize crosstalk, we are using probes from the company Senis which have small planar Hall effect[12]. Senis did not have "off the shelf" probes that would fit in the beam pipe, so they built custom probes for us with small packages for the Hall elements and miniature cables to get the signals out. Because these are the first such miniature probes Senis built, our options for the number and the positions of the Hall elements were limited. We chose to use probes with three elements measuring B_x, B_y, and B_z all along the same line, but offset in z. This is illustrated in figure 8. Corrections for the z-positions of the probes will be made in the analysis software. We could only fit two such probes in the beam pipe. We arranged them offset by 200 μm as shown in figure 9. We made the offset in the y direction. One probe is on the axis of the cylindrical assembly, and the other probe is 200 μm above the axis. The cables from the first probe must pass the other, and Senis engineered the pair to avoid potential interference.

[11] A similar arrangement was used by I. Vasserman, et al., "Comparison of Arepoc and Sentron Hall Sensors using Undulator A at the APS Magnetic Measurement Facility", presented by Y. Levashov at IMMW-17, Barcelona, September, 2011.

[12] D. Popovic, et al., "Three-Axis Teslameter With Integrated Hall Probe", IEEE Trans. Instr. Meas. 56, August, 2007, p. 1396.

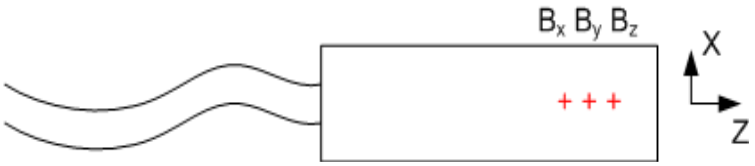

Figure 8: Three Hall probe elements measure the three field components along the line of motion of the probe.

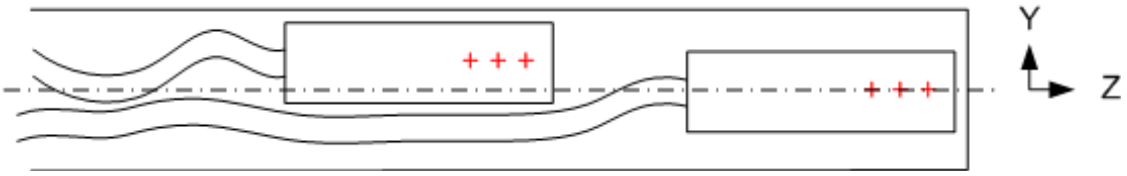

Figure 9: Two Hall probe packages are mounted offset in the y-direction in the assembly.

This orientation of the probes lets us determine the fields in the undulator at two points vertically offset. Rotating the probes by 90 degrees lets us determine the fields at two points horizontally offset.

6.2 Position Of The Magnetic Center Relative To The Probes

In the linear polarization modes, the x and y behavior of the fields are easily separated. This will let us use our two probes to measure at two points in either the x direction or the y direction and from these measurements determine the field variation parameter in that direction. We measure both B_x and B_y, in both the x direction and the y direction, giving four ways to get a determination of a relative magnetic center coordinate.

Suppose the undulator is in the vertical field mode. The general field behavior is illustrated in figure 10. Near the magnetic center, the x-dependence of B_x goes as a hyperbolic sine, and of B_y goes as a hyperbolic cosine. Since k_y is imaginary, near the magnetic center the y-dependence of B_x goes as sine, and the y-dependence of B_y goes as cosine. Only the rough shape of the fields is shown in the figure.

The fields were calculated above with the magnetic center at $x = 0$, $y = 0$. When the magnetic center is shifted to (x_c, y_c), the equations become

$$B_x = \phi_0 k_x \sinh\left[k_x\left(x - x_c(z)\right)\right] \sinh\left[k_y\left(y - y_c(z)\right)\right] \cos\left(k_u z\right) \quad (86)$$

$$B_y = \phi_0 k_y \cosh\left[k_x\left(x - x_c(z)\right)\right] \cosh\left[k_y\left(y - y_c(z)\right)\right] \cos\left(k_u z\right) \quad (87)$$

$$B_z = -\phi_0 k_u \cosh\left[k_x\left(x - x_c(z)\right)\right] \sinh\left[k_y\left(y - y_c(z)\right)\right] \sin\left(k_u z\right) \quad (88)$$

The simulation gives $k_x = 0.222$ 1/mm and $k_y = i0.129$ 1/mm. In what follows, we leave the hyperbolic sine or cosine form of the field variation in the y direction with complex k_y. This is equivalent to using a sine or cosine function with real k_y. Note that the magnitude of k_x is larger than the magnitude of k_y, which means the field varies more rapidly in x than in y.

6.2.1 $(x_1 - x_c)$ from B_x, Linear Polarization Vertical Field Mode

First consider B_x. Its x-dependence has the form

$$B_x = B_0(y, z)\ \sinh[k_x(x - x_c(z))] \quad (89)$$

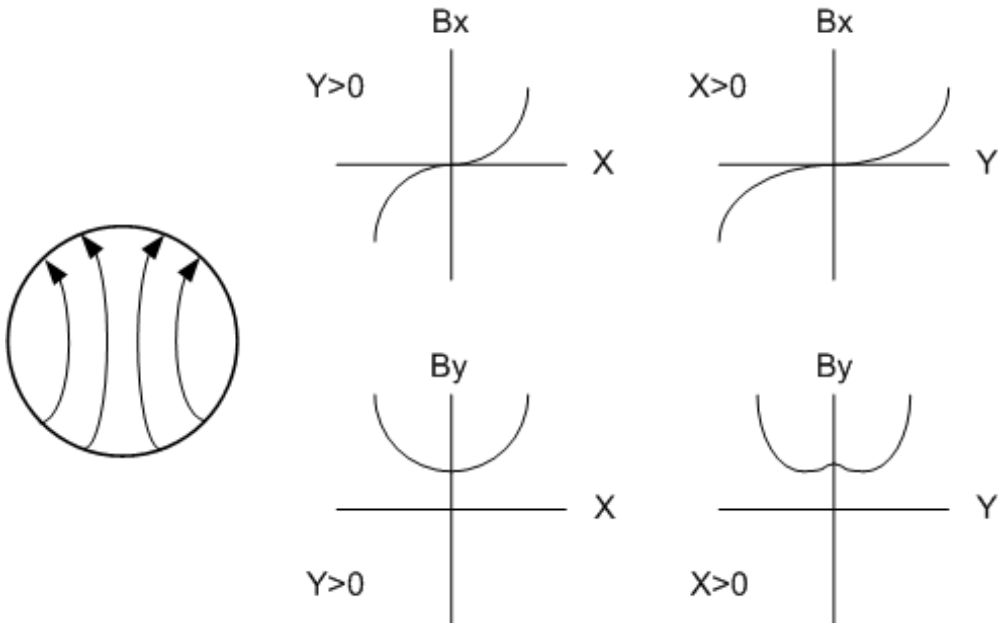

Figure 10: In linear polarization vertical field mode the field behaves in general as shown in these plots. Since k_y is imaginary, the curvature of the B_y vs y plot is concave down at the magnetic center.

If we turn the probe package 90° so that the two probes are shifted in x by $\Delta x = \Delta y$, probe 1 measures

$$B_{x1} = B_0 \sinh[k_x(x_1 - x_c(z))] \tag{90}$$

and probe 2 measures

$$B_{x2} = B_0 \sinh[k_x(x_1 + \Delta x - x_c(z))] \tag{91}$$

We measure very close to the magnetic center so that $|k_x(x - x_c(z))| << 1$. In this case, we use the linear term in the expansion of the field.

$$B_{x1} \simeq B_0 k_x(x_1 - x_c(z)) \tag{92}$$

$$B_{x2} \simeq B_0 k_x(x_1 + \Delta x - x_c(z)) \tag{93}$$

Solving for $x_1 - x_c(z)$, we find

$$(x_1 - x_c(z)) = \frac{B_{x1}}{B_{x2} - B_{x1}} \Delta x \tag{94}$$

All quantities on the right side are known. This gives the x-position of the magnetic center if we know the position of probe 1. Furthermore, it does not depend on the value of k_x. The method is illustrated in figure 11. One potential problem occurs if the probes are at $y = y_c$, in which case the measured fields go to zero. Another determination of $x_1 - x_c$ would then be made.

6.2.2 $(y_1 - y_c)$ from B_x, Linear Polarization Vertical Field Mode

Now suppose we turn the probe package to its normal configuration where the probes are shifted by Δy. Then B_x has y-dependence of the form

$$B_x = B_0(x, z) \sinh[k_y(y - y_c(z))] \tag{95}$$

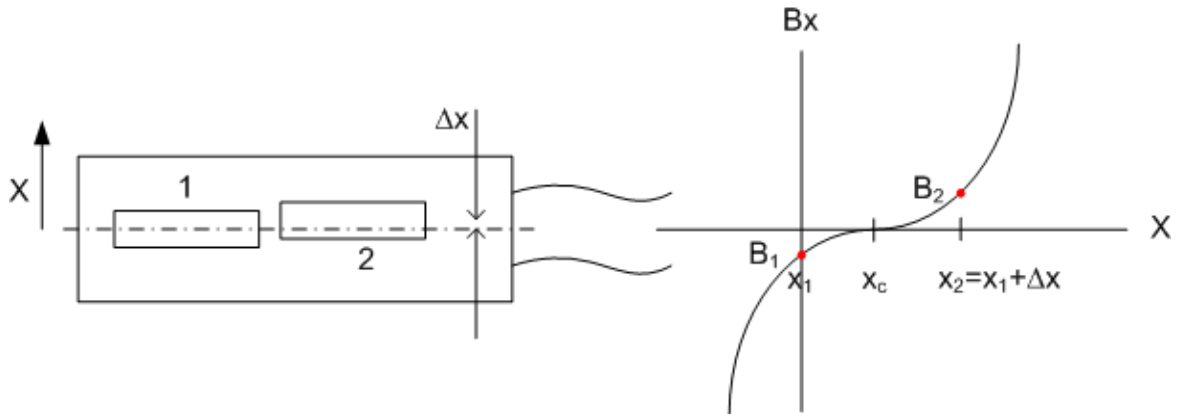

Figure 11: Two measurements of B_x allow the x-position of the magnetic center to be found.

Again we measure close to the magnetic center so $|k_y(y - y_c(z))| << 1$. We use a linear expansion of the field to determine the two measured B_x fields from probes 1 and 2.

$$B_{x1} \simeq B_0 k_y(y_1 - y_c(z)) \tag{96}$$
$$B_{x2} \simeq B_0 k_y(y_1 + \Delta y - y_c(z)) \tag{97}$$

Solving for $y_1 - y_c(z)$, we find

$$(y_1 - y_c(z)) = \frac{B_{x1}}{B_{x2} - B_{x1}} \Delta y \tag{98}$$

This gives a determination of the magnetic center y-position which does not depend on the value of k_y. This measurement works well as long as $x \neq x_c$, in which case the measured fields are zero and another method must be used.

6.2.3 $(x_1 - x_c)$ from B_y, Linear Polarization Vertical Field Mode

Now consider B_y. Its x-dependence has the form

$$B_y = B_0(y, z)\ \cosh[k_x(x - x_c(z))] \tag{99}$$

If we turn the probe package 90° so that the two probes are shifted in x by $\Delta x = \Delta y$, probe 1 measures

$$B_{y1} = B_0 \cosh[k_x(x_1 - x_c(z))] \tag{100}$$

and probe 2 measures

$$B_{y2} = B_0 \cosh[k_x(x_1 + \Delta x - x_c(z))] \tag{101}$$

We measure very close to the magnetic center so that $|k_x(x - x_c(z))| << 1$. In this case, we use the quadratic expansion of the field.

$$B_{y1} \simeq B_0 \left\{1 + \frac{1}{2} k_x^2 (x_1 - x_c)^2\right\} \tag{102}$$
$$B_{y2} \simeq B_0 \left\{1 + \frac{1}{2} k_x^2 \left[(x_1 - x_c)^2 + 2(x_1 - x_c)\Delta x + \Delta x^2\right]\right\} \tag{103}$$

Solving for $x_1 - x_c(z)$, we find

$$(x_1 - x_c(z)) = \frac{B_{y2} - B_{y1}}{B_{y1}} \frac{1}{k_x^2 \Delta x} - \frac{1}{2}\Delta x \tag{104}$$

All quantities on the right side except k_x are known. To find the magnetic center relative to probe 1, we can use the value of k_x from the model. We would use this calculation if the method presented in the previous section does not work because $y = y_c$ and $B_0 = 0$. Alternatively, we can use the magnetic center position determined above using B_x and this expression to determine k_x. This will be done below. The method is illustrated in figure 12.

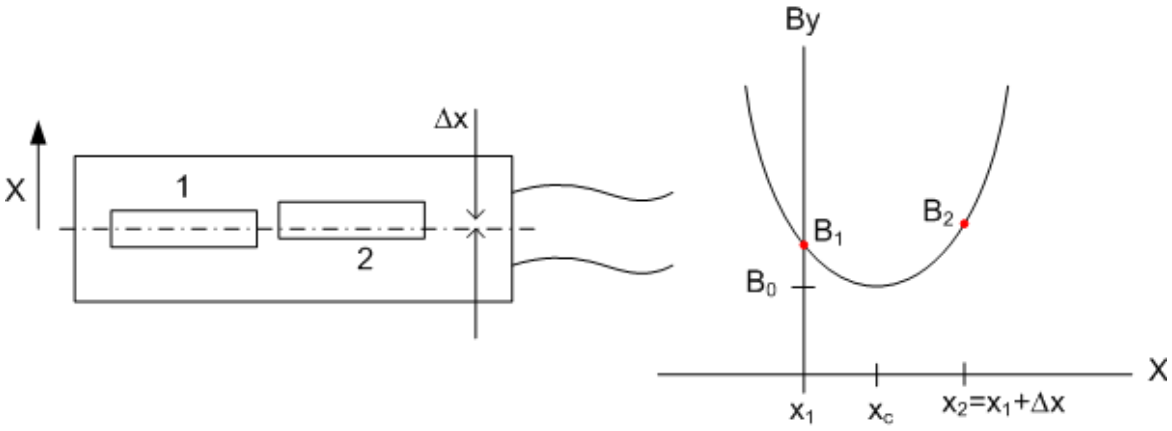

Figure 12: Two probes allow determination of the position of the magnetic center relative to the probes.

6.2.4 $(y_1 - y_c)$ from B_y, Linear Polarization Vertical Field Mode

Finally, suppose we orient the probes back to their vertical configuration and measure B_y at two points. B_y's y-dependence has the form

$$B_y = B_0(x, z)\ \cosh[k_y(y - y_c(z))] \tag{105}$$

Expanding the field to second order and finding its values at the positions of probe 1 and probe 2, we have

$$B_{y1} \simeq B_0 \left\{ 1 + \frac{1}{2} k_y^2 (y_1 - y_c)^2 \right\} \tag{106}$$

$$B_{y2} \simeq B_0 \left\{ 1 + \frac{1}{2} k_y^2 \left[(y_1 - y_c)^2 + 2(y_1 - y_c)\Delta y + \Delta y^2 \right] \right\} \tag{107}$$

Solving for $y_1 - y_c(z)$, we find

$$(y_1 - y_c(z)) = \frac{B_{y2} - B_{y1}}{B_{y1}} \frac{1}{k_y^2 \Delta y} - \frac{1}{2}\Delta y \tag{108}$$

This expression gives the y-position of the magnetic center relative to probe 1 provided we know k_y. Alternatively, we can find k_y if we know the relative magnetic center position.

6.2.5 Linear polarization horizontal field

The above procedure can be repeated with the undulator in linear polarization horizontal field mode. The equations giving the magnetic center position relative to probe 1 are identical to those given above except with x and y interchanged.

In total, we have four determinations of $(x_1 - x_c(z))$ and four determinations of $(y_1 - y_c(z))$. Two determinations of each involve a k parameter. The consistency of these measurements will be studied. We will also use these equations to determine the k parameters.

We determine the position of probe 1, (x_1,y_1), below. This allows us to determine the position of the magnetic center since we know its position relative to probe 1.

6.3 Determine k_x and k_y

When using the undulator mode with linear polarization vertical field, we had two expressions for $(x_1 - x_c(z))$, one of which involved k_x. Using B_x, we found

$$(x_1 - x_c(z)) = \left[\frac{B_{x1}}{B_{x2} - B_{x1}}\right]_x \Delta x \tag{109}$$

where we explicitly say, using the subscript on the bracket, that the B_x measurements were made with the probes in the x-direction. Using B_y, we found

$$(x_1 - x_c(z)) = \left[\frac{B_{y2} - B_{y1}}{B_{y1}}\right]_x \frac{1}{k_x^2 \Delta x} - \frac{1}{2}\Delta x \tag{110}$$

where we explicitly say that the B_y measurements were made with the probes in the x-direction. We point out that both B_x and B_y are measured in the same scan of the undulator so indeed $(x_1 - x_c(z))$ is the same in both expressions. When we equate these expressions for the relative magnetic center position, we can calculate the value of k_x. We find

$$k_x^2 = \frac{1}{\Delta x^2} \frac{\left[\frac{B_{y2}-B_{y1}}{B_{y1}}\right]_x}{\left[\frac{B_{x1}}{B_{x2}-B_{x1}}\right]_x + \frac{1}{2}} \tag{111}$$

In a similar way, we had two expressions for $(y_1 - y_c(z))$. Using B_x, we found

$$(y_1 - y_c(z)) = \left[\frac{B_{x1}}{B_{x2} - B_{x1}}\right]_y \Delta y \tag{112}$$

where we explicitly say, using the subscript on the bracket, that the B_x measurements were made with the probes in the y-direction. Using B_y, we found

$$(y_1 - y_c(z)) = \left[\frac{B_{y2} - B_{y1}}{B_{y1}}\right]_y \frac{1}{k_y^2 \Delta y} - \frac{1}{2}\Delta y \tag{113}$$

where we explicitly say that the B_y measurements were made with the probes in the y-direction. Both B_x and B_y are measured in the same scan of the undulator so $(y_1 - y_c(z))$ is the same in both expressions. When we equate these expressions for the relative magnetic center position, we can calculate the value of k_y. We find

$$k_y^2 = \frac{1}{\Delta y^2} \frac{\left[\frac{B_{y2}-B_{y1}}{B_{y1}}\right]_y}{\left[\frac{B_{x1}}{B_{x2}-B_{x1}}\right]_y + \frac{1}{2}} \tag{114}$$

The same procedure will be followed using the horizontal field mode of the undulator. This will provide a check of the k_x and k_y values.

6.4 Probe Position Relative To A Straight Line

We know the position of the magnetic center relative to the position of probe 1. We now proceed to determine the position of probe 1. The probe will be located magnetically at two points outside the undulator, and the straight line between these two points will establish an axis for a coordinate system. Inside the undulator, we must determine how the probe motion deviates from a straight line. The line does not necessarily have to be the coordinate axis. Relating the probe position to different lines is easily done with a linear transformation.

We now find the probe position relative to a straight line through the undulator. For a straight line, we use a laser beam[13]. The technique is illustrated in figure 13. A corner cube is mounted at

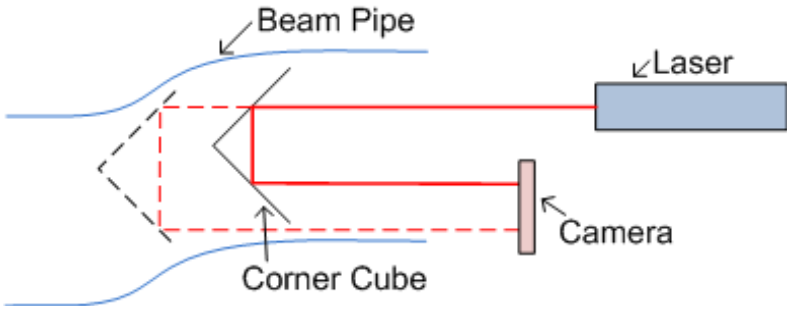

Figure 13: A corner cube reflects an incident laser beam back to a camera. The position of the beam at the camera depends on the transverse position of the corner cube as shown.

the end of the Hall probe package. A laser beam directed toward the probe package is reflected by the corner cube. The position of the reflected beam is measured on a camera. The reflected beam position depends on the transverse position of the corner cube. This technique gives changes in both the x and y positions of the Hall probe package relative to the straight line of the laser beam.

Suppose we place the laser at the entrance end of the undulator. At some position before the undulator, we define the position to be $z = 0$. At $z = 0$, we define the distance from the probe package to the laser beam to be $u = 0$ in the x-direction and $v = 0$ in the y-direction. This is illustrated for the x-direction in figure 14. As the probe assembly is moved through the undulator,

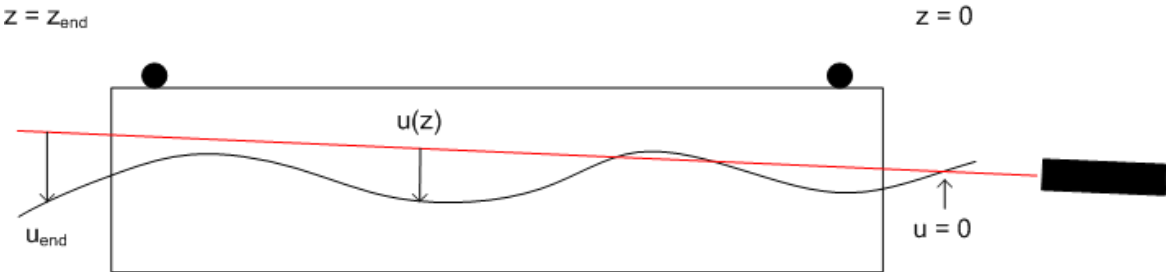

Figure 14: The position of the probe assembly is determined relative to the straight line of a laser beam.

the retroreflector system gives the changes in the x and y probe positions. We denote these as $(u(z), v(z))$. At a point outside the undulator, at $z = z_{end}$, the change in the probe assembly position relative to the laser beam and relative to the $z = 0$ point is (u_{end}, v_{end}).

[13] This work was done by Georg Gassner of SLAC.

In order to make this more concrete, suppose the laser system gives the coordinates of the reflected beam on a readout as U and V. At $z = 0$, we measure U_0 and V_0. Then

$$u(0) = U(0) - U_0 = 0 \quad (115)$$
$$u(z) = U(z) - U_0 \quad (116)$$
$$u_{end} = U(z_{end}) - U_0 \quad (117)$$
$$v(0) = V(0) - V_0 = 0 \quad (118)$$
$$v(z) = V(z) - V_0 \quad (119)$$
$$v_{end} = V(z_{end}) - V_0 \quad (120)$$

Note that $(u(z), v(z))$ should be the same whether the probe package is rotated or not.

6.5 Probe Position In A Fiducialized Coordinate System

The $(u(z), v(z))$ measurements tell us how the probes move through the undulator relative to a straight line. The next step is to determine where the probes are relative to an object that can be fiducialized so we can determine where the probes are in space. We do this magnetically at each end of the undulator. The probe positions at the two ends of the undulator give two points on a straight line. This is a natural axis for a coordinate system since only straightness corrections must be made. Further transformations to the mechanical center line of the undulator or to tooling balls on the undulator can be done at a later time.

The technique for locating the y-position of Hall probe 1 at each end of the undulator is illustrated in figure 15. Fiducialization magnets are placed at each end of the undulator at the $z = 0$ and the

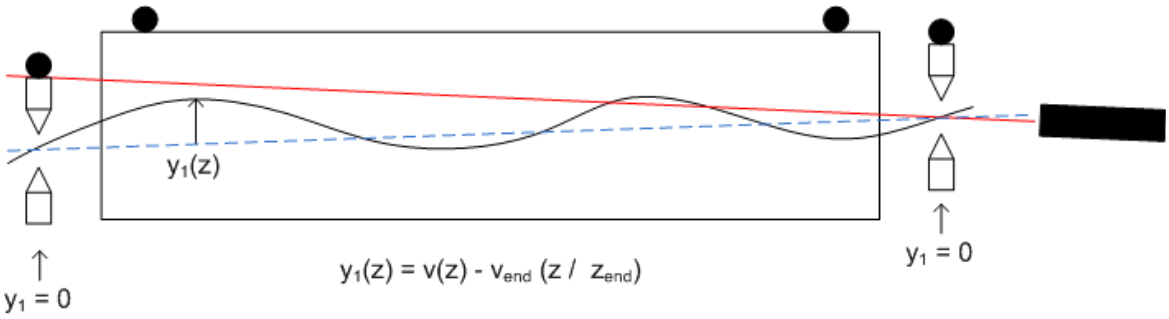

Figure 15: Fiducialization magnets are used to locate the Hall probes at each end of the undulator.

$z = z_{end}$ locations. Fiducialization magnets are magnetized cones with the same magnetic polarity mounted in a fixture with tooling balls on the outside of the fixture. The fixture allows the assembly to be flipped in a kinematic mount so the zero field point can be located relative to the tooling balls. The fiducialization magnets are described more fully in an LCLS technical note[14]. In particular, the note describes the calibration procedure which allows the position of the magnetic center of the fiducialization magnet to be determined relative to the tooling balls.

At $z = 0$, we move the fiducialization magnet until Hall probe 1 is at the magnetic center. From the calibration, the position of Hall probe 1 relative to the tooling balls on the fiducialization magnet is then known at the entrance end. At $z = z_{end}$, we move that fiducialization magnet until Hall probe 1 is at the magnetic center, and then the position of Hall probe 1 is known relative to the tooling balls on the fiducialization magnet at the exit end.

[14] Y. Levashov and Z. Wolf, "Test of Magnetic Transfer From Magnetic to Mechanical Reference for LCLS Undulator Fiducialization", LCLS-TN-05-10, April, 2005.

We define a line between the probe 1 positions at each end of the undulator as our measurement coordinate axis. Let $(x_1(z), y_1(z))$ be the position of Hall probe 1 relative to this line. At $z = 0$ and at $z = z_{end}$, $(x_1, y_1) = (0, 0)$. We now transfer our knowledge of the probe position relative to the laser line to the probe position relative to this new line. The linear transformation is

$$x_1(z) = u(z) - u_{end}\frac{z}{z_{end}} \quad (121)$$

$$y_1(z) = v(z) - v_{end}\frac{z}{z_{end}} \quad (122)$$

This tells us the position of Hall probe 1 at any point in the undulator relative to a line which can be located by tooling balls. We will use the position of the line between the two probe positions, which is the same as the line between the magnetic center's of the fiducialization magnets, as the $x = 0$, $y = 0$ line of our measurement coordinate system. This coordinate system, and the ideal beam axis in this coordinate system, will be related to tooling balls on the undulator.

When the probe assembly is rotated, the position of probe 1 changes due to errors in constructing the probe assembly. This is illustrated in figure 16. The (u, v) coordinates should remain the same

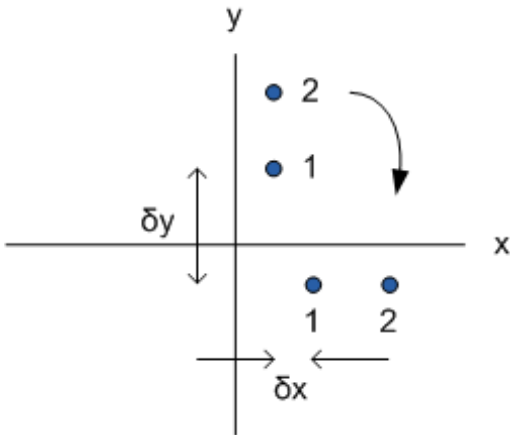

Figure 16: Probe 1 and probe 2 positions when the assembly is oriented vertically and horizontally. The axes indicate the center of rotation.

when a measurement is done with the rotated probe, but the fiducialization magnets will locate probe 1 at positions shifted by δx and δy as shown in the figure. We will use the positions of probe 1 in the vertical orientation at each end of the undulator to define the coordinate system. When we use the probe with horizontal orientation, we will apply the $(\delta x, \delta y)$ correction to the position of probe 1.

6.6 Determine The Beam Axis

We now determine the position of the magnetic center through the undulator relative to our coordinate system. We know the position of the magnetic center relative to probe 1 from equation 94 giving $(x_1 - x_c)$ and equation 98 giving $(y_1 - y_c)$. This gives us the position of the magnetic center as

$$x_c = x_1 - (x_1 - x_c) \quad (123)$$

$$y_c = y_1 - (y_1 - y_c) \quad (124)$$

Inserting the position of probe 1 from equation 121, we find

$$x_c(z) = u(z) - u_{end}\frac{z}{z_{end}} - (x_1(z) - x_c(z)) \quad (125)$$

$$y_c(z) = v(z) - v_{end}\frac{z}{z_{end}} - (y_1(z) - y_c(z)) \quad (126)$$

This is illustrated in the y-direction in figure 17.

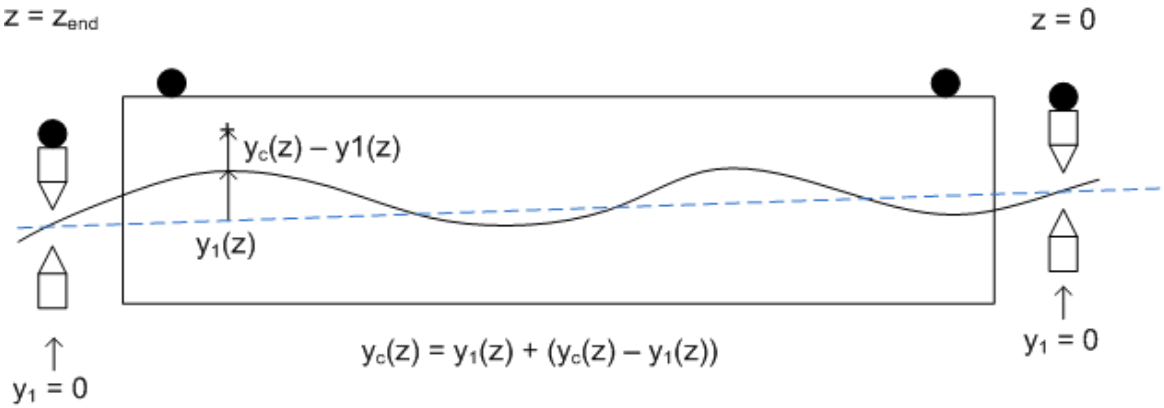

Figure 17: The position of the magnetic center is determined in the fiducialized coordinate system.

We now know the position of the center of the magnetic field at all points along the undulator in a coordinate system defined by tooling balls. We fit the magnetic center position curve with a straight line to determine the beam axis. This is illustrated in the y-direction in figure 18. The ends

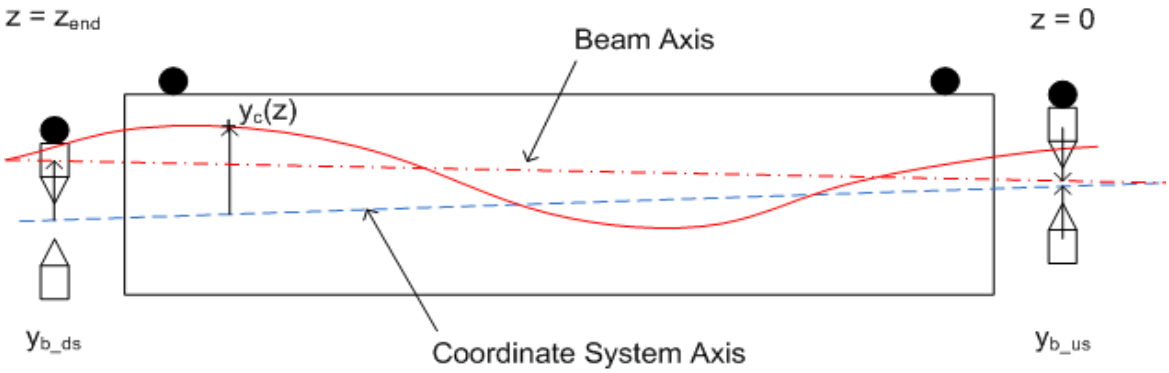

Figure 18: The magnetic center position is fit by a line to determine the beam axis.

of the beam axis line are denoted as (x_{b_us}, y_{b_us}) at the upstream end at $z = 0$, and (x_{b_ds}, y_{b_ds}) at the downstream end at $z = z_{end}$. These two points determine the beam axis in our coordinate system.

6.7 Fiducialization Of The Beam Axis

We now wish to determine the beam axis relative to tooling balls on the undulator. The undulator will have tooling balls on its top directly above the beam axis and on the side directly across from

the beam axis. These are used to align the undulator. We locate the beam axis relative to these tooling balls. The procedure is outlined for the y-direction in figure 19. At the upstream end of

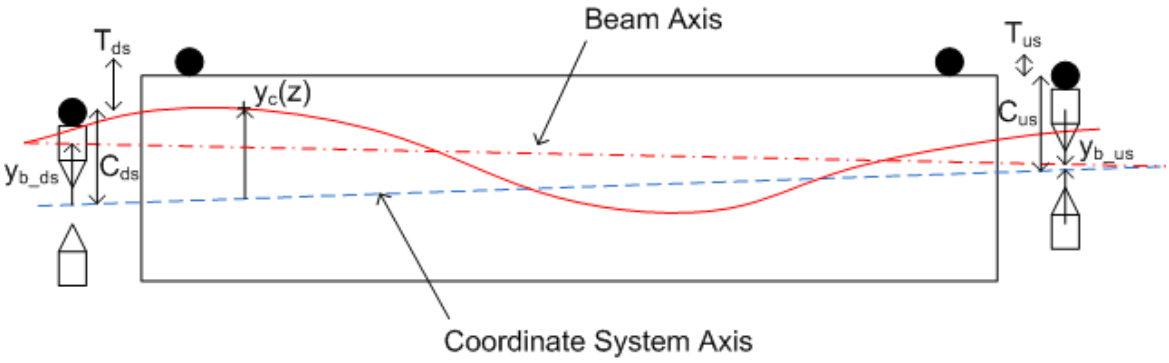

Figure 19: The beam axis is fiducialized by adding the distance from the undulator tooling balls to the fiducialization magnet tooling balls, the calibration of the fiducialization magnets, and the position of the beam axis relative to the center of the fiducialization magnets.

the undulator, the vertical distance of the beam axis below the undulator tooling ball is Y_{us} given by

$$Y_{us} = T_{us} + C_{us} - y_{b\_us} \tag{127}$$

In this equation, T_{us} is the distance from the undulator tooling ball to the tooling ball on the fiducialization magnet. C_{us} is the distance of the center of the fiducialization magnet from the upper tooling ball on it. This is determined in a calibration. y_{b_us} is the y-position of the beam axis at the fiducialization magnet. The y_{b_us} term is subtracted since the other terms refer to a distance measured down from the tooling balls, and the y_{b_us} term refers to the y-position measured positive up. A similar relation exists for the x-direction.

Similarly, at the downstream end, the distance of the beam axis down from the undulator tooling ball is

$$Y_{ds} = T_{ds} + C_{ds} - y_{b\_ds} \tag{128}$$

with a similar relation for X_{ds}. The upstream and downstream locations of the beam axis relative to tooling balls on the undulator completes the fiducialization of the beam axis.

6.8 Trajectories, Phase, K Value

Using the procedure detailed in the previous sections, we have determined the beam axis, and we know where our probe is relative to the beam axis. We now take the field components measured by probe 1, which is nominally on the axis of the probe package, and from them calculate the fields on the beam axis. Once we determine the fields on the beam axis, we can calculate the trajectories, phase, and K value.

The two probes in the assembly do not provide enough information for a fit to determine the fields on the beam axis. A larger assembly of probes, at least three in the x-direction and three in the y-direction, would be needed to do a second order fit to the measurements in order to use the fit to determine the fields on the beam axis. This is an area for future development.

Using the probes available, we determine the fields on the beam axis as follows. We know the measured fields at the known position of probe 1, and we know the position of the beam axis. We use the analytic expression for the field behavior as a function of position in order to calculate the fields on the beam axis given the measurements. We assume that probe 1 is within 200 μm of

the beam axis accounting for tolerances in assembling the undulator and the probe package, and accounting for required clearances between the components. Since this distance is small, we will make small corrections to the probe 1 measurements to give the fields on the beam axis. We can use the functional form of the fundamental term in the field expansion to make the corrections since the errors from the higher field harmonics will make second order corrections. We know the values of the k parameters. The unknown is the field value at the magnetic center, an overall scale factor. We calculate it from the measurement.

In all cases above, the fields had the form

$$B_i = B_{i0} f_i(x, y, z) \tag{129}$$

where $i = x$, y, or z, and f is a function which depends on the polarization mode and whose form was given explicitly for the linear and circular polarization modes. The field component measured by probe 1 is

$$B_{i1} = B_{i0} f_i(x_1 - x_c, y_1 - y_c, z) \tag{130}$$

where (x_c, y_c) are the coordinates of the magnetic center, (x_1, y_1) are the coordinates of probe 1, and $i = x$, y, or z. The field amplitude at the magnetic center is then

$$B_{i0} = \frac{B_{i1}}{f_i(x_1 - x_c, y_1 - y_c, z)} \tag{131}$$

We want the field on the beam axis. This is given by

$$B_{ib} = B_{i0} f_i(x_b - x_c, y_b - y_c, z) \tag{132}$$

where (x_b, y_b) are the coordinates of the beam axis. The fields on the beam axis are then given by

$$B_{ib} = \frac{B_{i1}}{f_i(x_1 - x_c, y_1 - y_c, z)} f_i(x_b - x_c, y_b - y_c, z) \tag{133}$$

All quantities on the right hand side are known including k_x and k_y, and x_c and y_c in all polarization modes.

This technique uses the measured field and the functional form of the field dependence with position to determine the field on the beam axis. It assumes that the fundamental term in the field expansion is dominant, that the field measurement is near the magnetic center and near the beam axis so corrections are small, and that higher harmonics in the field contribute second order terms to the small correction of the measured field.

One can consider using the second probe to refine this technique, or as a check. One can also consider making a larger probe array, fitting the measurements, and then interpolating to determine the fields on the beam axis. The errors associated with using a single measurement and the functional form of the field must be studied. These are areas for future development.

7 Conclusion

A measurement plan for the Delta undulator was presented. The field integrals are measured using two techniques which use a single wire. The techniques involved first moving the wire and second sending a current pulse down the wire. A plan was then presented to make point measurements of the fields in the undulator. Two Hall probes were used in an assembly. The two measurements allowed a determination of the magnetic center position relative to the probes when the undulator was in vertical planar field mode and horizontal planar field mode. The constants determining the field dependence on x and y, k_x and k_y, are determined by these measurements. The position of the probes was determined using a laser system and fiducialization magnets. The combination of

knowing the probe position and the magnetic center position relative to the probe gives the magnetic center position. Knowing the magnetic center as a function of z, a linear fit was used to determine the beam axis. Once the beam axis was known, the fields on the beam axis were determined by correcting the measured field using the functional form of the field dependence with position and the known positions of the measurement, the magnetic center, and the beam axis. Knowing the fields on the beam axis allows one to calculate the trajectories, phase, and K value.

Acknowledgements
I am grateful to Heinz-Dieter Nuhn, Yurii Levashov, Scott Anderson, and Alexander Temnykh for many discussions about this work.